Spectroscopy of $LiTaO_3:Pr^{3+}$ crystals

1997 J. Phys.: Condens. Matter 9 5217

(http://iopscience.iop.org/0953-8984/9/24/018)

J. Phys.: Condens. Matter **9** (1997) 5217–5227. Printed in the UK PII: S0953-8984(97)77844-5

Spectroscopy of $LiTaO_3$: Pr^{3+} crystals

I Sokólska†, W Ryba-Romanowski†, S Gołąb†, T Łukasiewicz‡ and M Świrkowicz‡

† W Trzebiatowski Institute of Low Temperature and Structure Research, Polish Academy of Sciences, 50-950 Wrocław 2, PO Box 937, Poland
‡ Institute of Electronic Materials Technology, Warsaw, Poland

Received 16 September 1996, in final form 21 March 1997

Abstract. The polarized absorption spectra, time-resolved emission spectra, and emission lifetimes of Pr^{3+} doped $LiTaO_3$ crystals were measured. An intense emission from the $^3P_0$ level was observed. The positions of the Pr^{3+} levels, experimental oscillator strengths, and branching ratios from the $^3P_0$ and $^1D_2$ levels were determined. The results are discussed in terms of the Judd–Ofelt parameters.

1. Introduction

In the past years interest in crystals of $LiXO_3$ (X = Nb, Ta) type doped with rare earth or transition metal ions has significantly grown, as they can offer simultaneously nonlinear effects and lasing ability. $LiNbO_3$ and $LiTaO_3$ belong to the $R3c$ space group and are ferroelectric crystals with large electro-optic and nonlinear coefficients [1, 2]. They can be obtained either as good quality bulk crystals by the Czochralski method or as thin films by laser ablation [3], molecular beam epitaxy (MBE) [4], metalorganic chemical vapour deposition (MOCVD) [5], aerosol processes [6], and the sol–gel technique [7]. This makes them promising materials for waveguides and devices for integrated optoelectronics. Although the nonlinear coefficient d_{31} which determines the intensity of observed nonlinear effects is much less for $LiTaO_3$ than for $LiNbO_3$, the advantage of the $LiTaO_3$ crystal is its lower birefringence and considerably higher threshold for photorefractive damage [8]. Moreover, the method of quasi-phase-matching (QPM) [9] permits second-harmonic generation (SHG) and optical parametric oscillation (OPO) to be achieved taking advantage of the same order of magnitude of the d_{33} coefficient for both $LiNbO_3$ and $LiTaO_3$. A number of papers are concerned with optical and laser properties of $LiNbO_3$ crystals doped with rare earth and transition metal ions (e.g. [10]–[16]). Fewer papers [16–20] have been devoted to the spectroscopic properties of $LiTaO_3$ crystals, doped as yet mainly with Nd^{3+}.

In this paper we present the optical properties of Pr^{3+}-doped $LiTaO_3$ crystals such as polarized absorption, luminescence lifetimes, and time-resolved emission in the temperature range 4.2–300 K. We have analysed absorption spectra according to the selection rules for the symmetry expected for the dopant site and calculated the emission transition rates using the modified Judd–Ofelt theory. In spite of the similarity in the crystal and electronic structures of $LiTaO_3$ and $LiNbO_3$ crystals [21], we have found that the optical properties of the Pr^{3+} ion in $LiTaO_3$ differ significantly from those in the $LiNbO_3$ host [14].

0953-8984/97/245217+11$19.50

2. Experimental details

Crystals of $LiTaO_3:Pr^{3+}$ were grown by the Czochralski method from a congruent melt ($Li/Ta = 0.94$) with a different amount of Pr_2O_3 as a dopant. The concentrations of Pr^{3+} in the crystals investigated in this work, estimated by chemical analysis and by measurements of the absorption coefficient, were about 0.4 mol% (1.27×10^{20} ions cm^{-3}) and 0.05 mol% (1.6×10^{19} ions cm^{-3}). All measurements were made with samples oriented along the crystallographic axes. Absorption spectra were measured with a Varian 2300 absorption spectrophotometer. Luminescence spectra and decay kinetics were obtained after excitation by a nitrogen-pumped tunable dye laser ($\lambda_{max} = 460$ nm, 10 Hz, 8 ns pulse) with a setup consisting of a grating monochromator (Zeiss GDM 1000), a photomultiplier, a SRS 250 boxcar integrator, and a personal computer. A calibrating tungsten lamp (Osram Wi17/G) operating at 1600 K was used to correct the luminescence spectra for the spectral resolution and sensitivity of the apparatus. For measurements in the 4.2–300 K range the crystals were cooled in a continuous-flow helium cryostat (Oxford CF 1204) with a temperature controller.

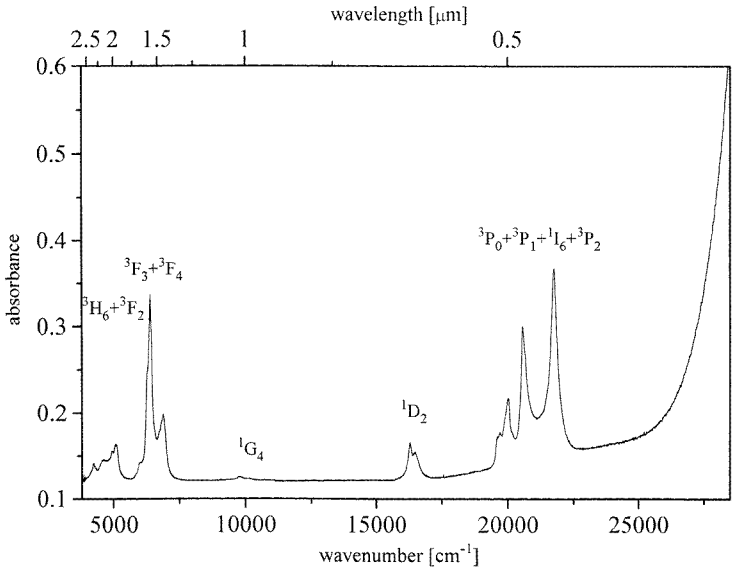

Figure 1. The absorption spectrum of the $LiTaO_3:Pr^{3+}$ (0.4 mol% Pr^{3+}, $d = 0.2$ cm) crystal measured at 300 K.

3. Results and discussion

In figure 1 the absorption spectrum of the $LiTaO_3:Pr^{3+}$ crystal investigated (0.4 mol% Pr^{3+}) recorded at room temperature is shown. In the spectrum five groups of bands corresponding to the intraconfigurational $4f^2 \rightarrow 4f^2$ transitions from the $^3H_4$ ground state to the higher multiplets of the trivalent praseodymium ion are observed. Except for the absorption edge there is no significant increase of absorbance due to the crystal matrix as was observed by the authors of [14] or [17] for wavelengths shorter than 600 or 450 nm for $LiNbO_3$ or $LiTaO_3$ crystals, respectively. The intensities of the praseodymium absorption bands

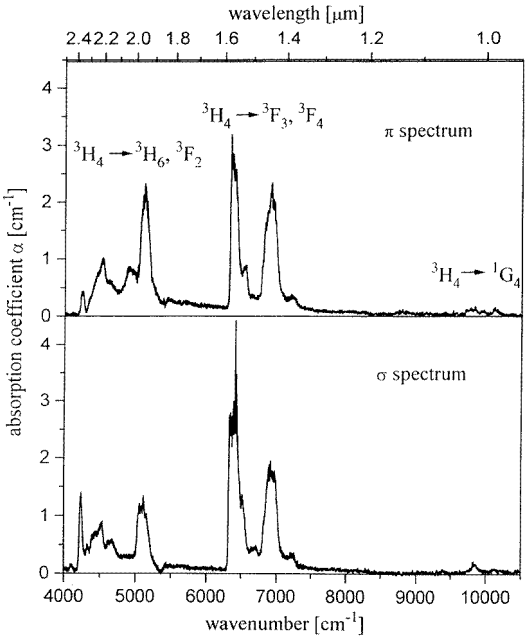

Figure 2. IR absorption spectra of the $LiTaO_3$: Pr^{3+} (0.4 mol% Pr^{3+}) crystal measured at 4.2 K for the incident light polarized parallel (π-spectrum) and perpendicular (σ-spectrum) to the *c*-axis of the crystal.

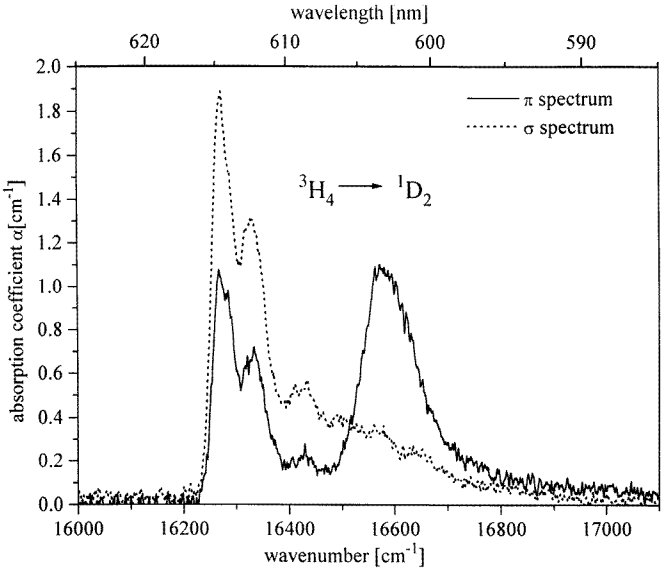

Figure 3. $^3H_4 \rightarrow {}^1D_2$ absorption bands of Pr^{3+} in the $LiTaO_3$: Pr^{3+} crystal measured at 4.2 K.

depend on the polarization of the incident light (figures 2–4) and are listed in table 1. The structure observed within the bands is due both to the splitting of the multiplets into Stark components and to the presence of different Pr^{3+} sites which are affected by a varying

crystal field strength. The lattice location of trivalent dopants in crystals of $LiXO_3$ (X = Nb, Ta) type has been studied by various techniques such as electron microprobe (EMP) [11], site selective spectroscopy (SSS) [15], Rutherford backscattering spectrometry (RBS) [15], electron paramagnetic resonance (EPR) [16], x-ray or neutron scattering [22], and x-ray standing-wave measurements [23]. Although there is still no definitive assignment, the results of x-ray standing-wave measurements, SSS and RBS obtained for the $LiNbO_3:Pr^{3+}$ crystal [14, 15] suggest that the praseodymium ions enter some off-centred Li octahedral sites. In this paper the structure of the $^3H_4 \rightarrow {}^3P_0$ absorption band at low temperature (figure 4) gives evidence for the presence of different Pr^{3+} sites in the $LiTaO_3$ crystal. Although the $^3P_0$ term does not split in the crystal field, the above band can be resolved into at least four components (figure 4, inset) as it is also for the $LiNbO_3:Pr^{3+}$ crystal [14]. At 4.2 K the maxima and halfwidths (in parenthesis) of these components are 19 962 cm^{-1} (42 cm^{-1}), 19 998 cm^{-1} (5 cm^{-1}), 20 030 cm^{-1} (25 cm^{-1}), and 20 063 cm^{-1} (45 cm^{-1}).

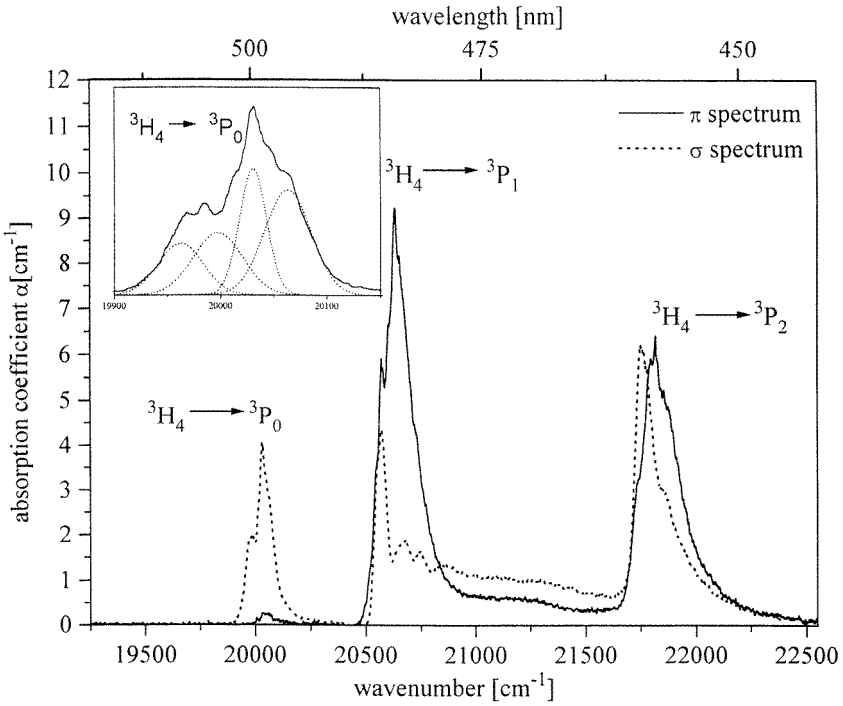

Figure 4. The absorption spectrum of the $^3H_4 \rightarrow {}^3P_0$, $^3P_1$, and $^3P_2$ transitions of Pr^{3+} in $LiTaO_3$ at 4.2 K. In the inset the decomposition of the $^3H_4 \rightarrow {}^3P_0$ absorption band into four Gaussian components is shown.

Assuming the Pr^{3+} ions to enter sites with C_3 local symmetry [14] we checked the consistency of polarized absorption spectra with the selection rules for electric-dipole transitions [24] given in table 2. The C_3 symmetry predicts three doubly degenerate E components and three A components of the ground $^3H_4$ multiplet. The $^3H_4 \rightarrow {}^3P_0$ absorption band significantly dominates in the σ-spectrum implying an E-type symmetry of the lowest level of the $^3H_4$ ground state. Unfortunately, this assumption fails in analysis of $^3H_4 \rightarrow {}^1D_2$, $^3H_4 \rightarrow {}^3P_1$, and $^3H_4 \rightarrow {}^3P_2$ transitions. Among other things we would expect that the transitions between E- and A- symmetry-type levels would appear only in

Table 1. Energies and absorption coefficients of the transitions observed in the polarized absorption spectra of Pr^{3+} in $LiTaO_3$ at 4.2 K.

	σ transitions ($E_\perp z$)		π transitions ($E_\parallel z$)	
Level	Energy (cm^{-1})	Absorption coefficient (cm^{-1})	Energy (cm^{-1})	Absorption coefficient (cm^{-1})
$^3H_6, ^3F_2$	3 907	0.57	3 908	0.36
	4109	0.15	4116	0.06
			4228	0.43
	4240	1.4	4247	0.43
	4330	0.49		
	4393	0.68		
	4435	0.73		
	4532	0.9	4532	1.0
	4632	0.55	4632	0.86
	4673	0.64		
			4898	0.86
	5061	1.22		
	5080	1.16		
	5114	1.3	5114	2.33
	5149	1.0		
	5439	0.19	5445	0.33
$^3F_3, ^3F_4$	6340	3.0	6341	3.09
			6363	2.85
	6410	4.42	6404	2.58
	6515	1.37	6530	0.84
	6707	0.48		
			6826	1.64
			6861	1.85
	6916	1.95	6913	2.34
	6976	1.68		
	7240	0.33	7240	0.33
$^1G_4$	9823	0.22	9837	0.18
	9852	0.18		
	10 110	0.10	10 110	0.10
$^1D_2$	16 270	1.89	16 270	1.1
	16 330	1.31	16 330	0.73
	16 434	0.57	16 430	0.26
			16 580	1.1
$^3P_0$	19 986	2.0		
	20 032	4.0	20 049	0.22
$^3P_1$	20 573	4.35	20 574	5.9
			20 634	9.23
	20 682	1.85		
	20 738	1.62		
	20 866	1.35		
$^3P_2$	21 756	6.2		
			21 740	3.2
			21 820	6.4
	21 867	2.96		

the σ-spectrum. However, the bands either are observed in both polarizations or dominate in the π-spectrum. The possible explanation of the inadequacy of the above selection rules could be the lowering of the C_3 site symmetry due to the charge compensating defects in the vicinity of Pr^{3+} ions.

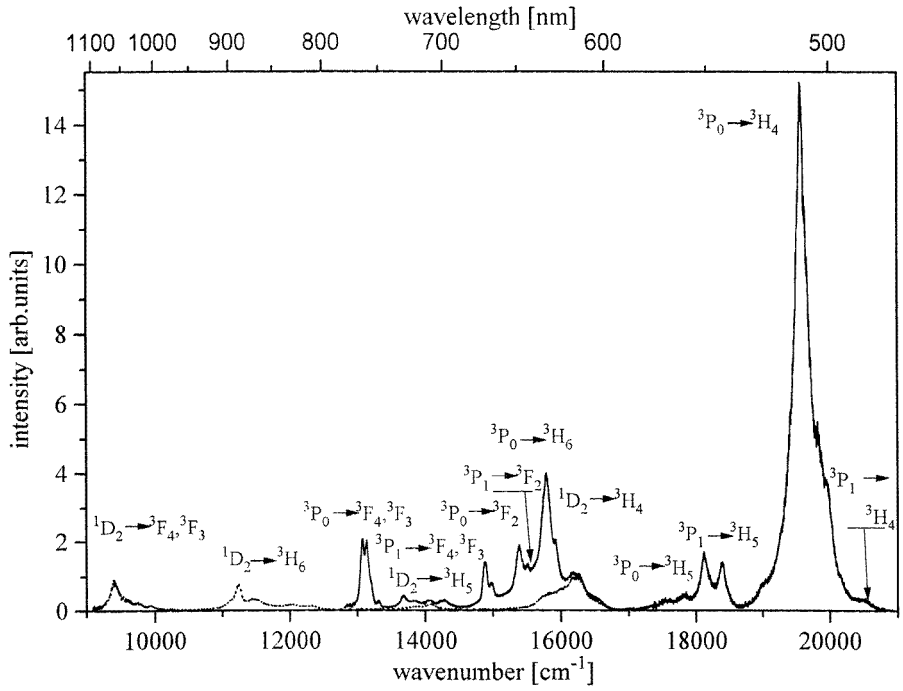

Figure 5. The $LiTaO_3:Pr^{3+}$ (0.4 mol%) luminescence spectrum measured at 300 K (λ_{exc} = 460 nm). The spectrum measured with a time delay of 5 μs is shown with a dotted line.

Table 2. Selection rules for electric-dipole transitions in the C_3 point group (from [24]).

	A	E
A	Z (π)	X, Y (σ)
E	X, Y (σ)	X, Y (σ), Z (π)

In figures 5–7 we present the luminescence of the $LiTaO_3:Pr^{3+}$ crystal following an excitation in the strong absorption band at 460 nm. A characteristic feature of the Pr^{3+} luminescence in this crystal is the strong emission from the $^3P_0$ level which was not observed for $LiNbO_3:Pr^{3+}$ [14]. The emission band in the range 18 700–20 100 cm^{-1} is due to the $^3P_0 \rightarrow {}^3H_4$ transitions. The low-temperature band can be decomposed into seven main Gaussian-shaped components (figure 7, inset). Their maxima determine the energies of the Stark components of the split $^3H_4$ ground state as 0, 127, 320, 425, 515, 690, and 990 cm^{-1}. Increasing the temperature from 4.2 to 300 K brings about a broadening of these components by around 40% and an increase of the relative intensities of low-energy components simultaneous with a decrease of the intermediate ones (figure 7). An additional weak band peaking at about 20 100 cm^{-1} occurs on the high-energy tail of the $^3P_0 \rightarrow {}^3H_4$ emission band with its intensity increasing as the temperature is raised. This band is probably related to the emission from the thermally populated $^3P_1$ multiplet, located at around 600 cm^{-1} above the $^3P_0$ state, to the ground $^3H_4$ state. The bands observed in the room-temperature spectrum (figure 5) between 13 800 and 14 500 cm^{-1}, at about 15 600 cm^{-1} and between 18 000 cm^{-1} and 18 600 cm^{-1} can also be attributed to the

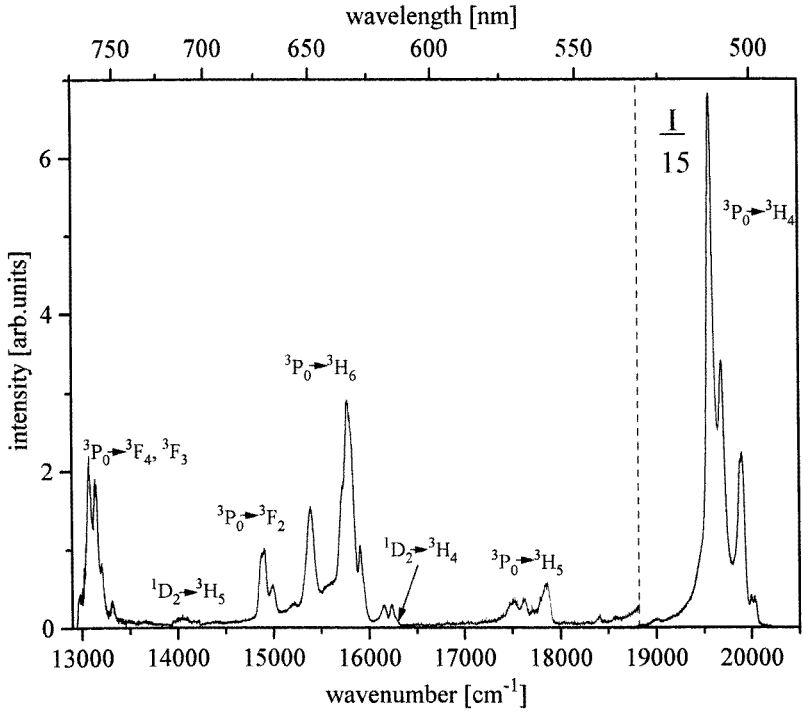

Figure 6. The $LiTaO_3$: Pr^{3+} (0.4 mol%) luminescence spectrum measured at 4.2 K (λ_{exc} = 460 nm). The intensity of the $^3P_0 \rightarrow {}^3H_4$ band is reduced 15-fold compared with the rest of the spectrum.

emission from the $^3P_1$ multiplet, as they are not observed in the low-temperature spectrum (figure 6). The bands in the emission spectrum around 14 000 cm^{-1} and between 15 500 and 16 800 cm^{-1} are attributed to the transitions from the $^1D_2$ multiplet. The assignment of these transitions was possible on the basis of lifetime measurements and time-resolved spectra. The lifetime of the $^3P_0$ level was estimated to be 0.48 μs for both samples independent of the praseodymium concentration while that of the $^1D_2$ level was estimated to be 50 and 17 μs for the samples with lower and higher concentrations, respectively. The luminescence spectrum measured with a time delay of 5 μs therefore reveals the emission from the $^1D_2$ level populated from the $^3P_0$ level and is shown in figure 5 (dotted line). The mechanism of the population of the $^1D_2$ level can not be decided explicitly yet. Both multiphonon relaxation and cross-relaxation processes cannot be excluded. The relative intensities of emission bands originating from the $^3P_0$ and $^1D_2$ levels depend on the concentration of the dopant and on the temperature. Taking into account the room-temperature spectrum in the region from 14 500 cm^{-1} to 16 800 cm^{-1}, the ratio of the integrated emission from the $^1D_2$ level to the integrated emission from the $^3P_0$ level is 1:2.1 for the sample with the higher concentration and 1:1.3 for the lower concentration. At 4.2 K these ratios are 1:5 and 1:3, respectively. The influence of the Pr^{3+} concentration on the relative $^1D_2/^3P_0$ intensity may be explained by the reduction of the quantum efficiency of the $^1D_2$ level due to the enhanced cross-relaxation processes in a concentrated sample, consistent with the shortening of the $^1D_2$ lifetime. Change of the relative $^1D_2/^3P_0$ intensity with the temperature together with a temperature-independent $^1D_2$ lifetime indicates that these two levels are

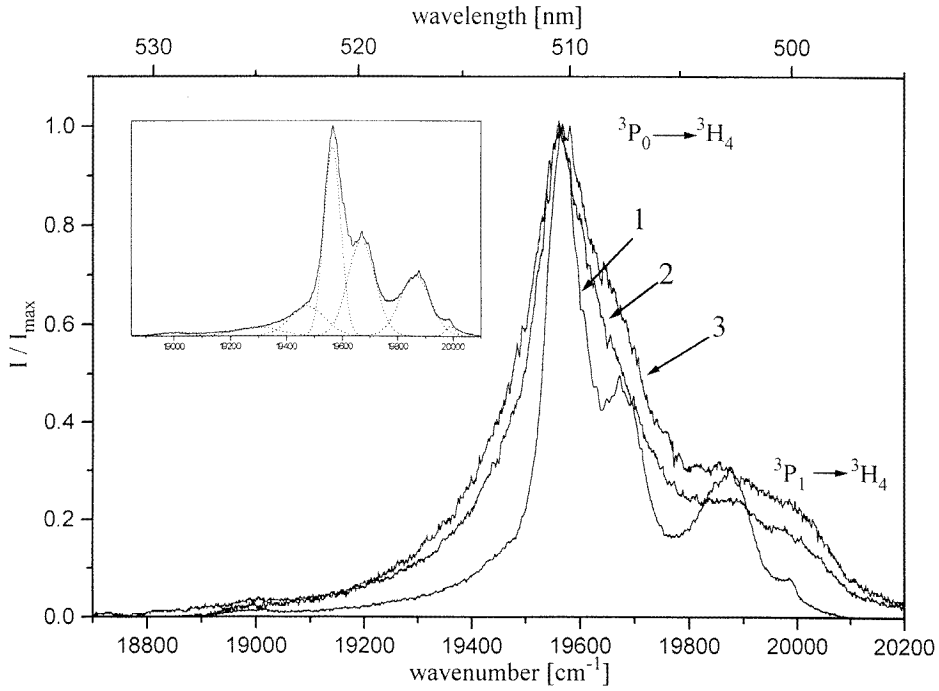

Figure 7. The $^3P_0 \rightarrow {}^3H_4$ luminescence spectra of Pr^{3+} in $LiTaO_3$ measured at 4.2 K (1), 230 K (2), and 300 K (3) ($\lambda_{exc} = 460$ nm). In the inset the decomposition of the 4.2 K spectrum into Gaussian components (dotted lines) is shown.

bridged by a temperature dependent relaxation process. The energy gap between $^3P_0$ and $^1D_2$ levels amounts to about 3400 cm^{-1} according to data in table 1. Lattice vibrations of $LiNbO_3$ and $LiTaO_3$ have been studied in a number of works (e.g. [25]–[27]). One of them [27] contains a detailed analysis of Raman spectra recorded with $LiNb_xTa_{1-x}O_3$ single crystals for x ranging from zero to unity. From this study it follows that the highest-energy vibrations correspond to a well defined band at 598 cm^{-1} in $LiTaO_3$ and to a broader band having two maxima of 580 and 630 cm^{-1} in $LiNbO_3$. Additional small features at 748 and 825 cm^{-1} in Raman spectra of $LiNbO_3$ have been attributed to a possible occurrence of $LiNbO_4$ phase [27]. Thus, at least four phonons are needed to bridge the $^3P_0 \rightarrow {}^1D_2$ energy gap. The energy gap law for the $LiTaO_3$ crystal has not been evaluated yet but abundant data on multiphonon relaxation in other rare-earth-doped oxide crystals indicate that the multiphonon relaxation rates involving simultaneous emission of four phonons are between 10^3 and 10^5 s^{-1}, depending on the electron–phonon coupling. It may be interesting to note here that a room-temperature luminescence lifetime of the $^4S_{3/2}$ level of Er^{3+} in $LiNbO_3$ amounting to 28 [28] or 32 [12] μs has been reported. The energy gap between the $^4S_{3/2}$ and the next lower-lying $^4F_{9/2}$ level is about 3000 cm^{-1} and the multiphonon relaxation rate for the $^4S_{3/2}$ level was estimated to be 2.8×10^4 s^{-1}. In our case, the praseodymium $^3P_0$ lifetime of 0.48 μs corresponds to a relaxation rate of 2.08×10^6 s^{-1} and the inclusion or subtraction of the multiphonon relaxation rate amounting to 10^5 s^{-1} would change the lifetime only by about 5%. Such a variation of lifetime is certainly beyond the experimental precision of our apparatus. Further measurements using a faster detection system will give more information on the temperature dependence of the $^3P_0$ lifetime. However, the question

of why the strongly luminescent $^3P_0$ level of Pr^{3+} in $LiTaO_3$ decays so quickly is still open. Also, the lack of the $^3P_0$ luminescence in $LiNbO_3$ [14] is not clear.

In order to estimate the rate of radiative transitions from the $^1D_2$ and $^3P_0$ multiplets we applied the classical Judd–Ofelt theory [29, 30] as well as the modified approach elaborated for the Pr^{3+} ion [31, 32]. The Judd–Ofelt parameters Ω_2, Ω_4, and Ω_6 and values of oscillator strengths (f_{calc} in table 3) were calculated numerically by the least-squares method using as input fitting parameters oscillator strengths calculated directly from the absorption spectrum (f_{meas} in table 3) [33]. In the analysis we have not taken into account the bands associated with the $^3H_4 \rightarrow {}^3F_2, {}^3H_6$ transitions, as their intensity was influenced by the accuracy limit of our spectrophotometer in this spectral range. In our case the Judd–Ofelt theory results in negative values for Ω_2, as often occurs for Pr^{3+}-doped materials. Only by neglecting the contribution from the $^3H_4 \rightarrow {}^3P_2$ transitions did the modified approach using the correction factor $\alpha = 1\times10^{-5}$ [31, 32] enable us to obtain positive values of Ω_2. The values for Ω_2, Ω_4, and Ω_6 are then calculated as 3.1×10^{-19} cm^2 ($\delta\Omega_2 = 35\%$), 0.6×10^{-19} cm^2 ($\delta\Omega_4 = 8\%$), and 0.56×10^{-19} cm^2 ($\delta\Omega_6 = 13\%$). The branching ratios calculated theoretically for the $^3P_0$ and $^1D_2$ levels using the above values of Ω_2, Ω_4, and Ω_6 (β_{calc}) are compared in table 4 with those determined from the emission spectrum (β_{meas}). Our measured branching ratios are similar to those observed by other authors for Pr^{3+} [34], whereas the calculated values completely differ from them. The radiative lifetimes calculated from these predicted values are 4.5 and 44 μs for the $^3P_0$ and $^1D_2$ levels, respectively. In spite of the relatively good agreement of the calculated and measured values of the $^1D_2$ lifetime, we have concluded that even the modified Judd–Ofelt approach is inadequate in our case and does not lead to a good consistence with the experiment. By doubling the value of the modification factor α it was possible to obtain a positive value for Ω_2 without neglecting the contribution from the $^3H_4 \rightarrow {}^3P_2$ transitions. However, the agreement between theoretically predicted and measured branching ratios was no better.

Table 3. Measured and calculated oscillator strengths for transitions from the ground $^3H_4$ state for Pr^{3+} ions in the $LiTaO_3$ crystal.

Final state	Mean transition energy (cm^{-1})	f_{meas} ($\times10^{-6}$)	f_{calc} ($\times10^{-6}$)
$^3P_0 + {}^3P_1 + {}^1I_6$	21 000	15.90	15.92
$^1D_2$	16 400	2.90	2.03
$^1G_4$	9800	0.40	0.48
$^3F_4$	6850	4.92	4.96
$^3F_3$	6300	10.1	10.1

We have also calculated the radiative transition rate w_{rad} for the $^1D_2 \rightarrow {}^3H_4$ transition, which is given [33] by

$$w_{rad} = \frac{f_{21}n}{1.51 \times 10^4 \lambda_0^2}\left(\frac{n^2+2}{3}\right)^2 = 5.75 \times 10^3 \ (\mathrm{s}^{-1}) \qquad (1)$$

where the severe approximations of the Judd–Ofelt theory are omitted. In the above equation f_{21} is the emission oscillator strength related to the absorption oscillator strength f_{12} by the reciprocity $f_{21} = (g_1/g_2)f_{12}$, g_1 and g_2 are degeneracies of the ground and excited states (we have assumed that the degeneracy is removed due to the symmetry, probably lower than C_3, and $g_1 = g_2 = 1$), λ_0 is the emission wavelength (in metres), and n is the refractive index of the material, equal to 2.18. As the observed emission transitions from the $^1D_2$ multiplet are not numerous and they are well separated in the emission spectrum, it was

possible to calculate the emission lifetime of the $^1D_2$ level using the branching ratios from the $^1D_2$ level to the $^3H_4$, $^3H_5$, $^3H_6$, and $^3F_4$ levels given in table 4. We finally obtained an emission lifetime of 61 μs for the $^1D_2$ level. The discrepancy between the calculated and experimental value (50 μs) may be due to the approximate character of the used reciprocity formula for f_{21}, where the partition functions inside each multiplet [35] were not taken into account. Applying (1) and this method for calculating the lifetime of the $^3P_0$ level was not reasonable, as we could not determine exactly the absorption oscillator strength for the $^3H_4 \rightarrow {}^3P_0$ transition.

Table 4. Measured and calculated branching ratios for transitions from the $^3P_0$ and $^1D_2$ levels of Pr^{3+} in the $LiTaO_3$ crystal. The values of the Judd–Ofelt parameters used for the calculations of β_{calc} are $\Omega_2 = 3.1 \times 10^{-19}$ cm^2, $\Omega_4 = 0.6 \times 10^{-19}$ cm^2, and $\Omega_6 = 0.56 \times 10^{-19}$ cm^2.

Transition	Mean transition energy (cm^{-1})	β_{meas}	β_{calc}
$^3P_0 \rightarrow {}^3F_4, {}^3F_3$	13 200	0.11	0.038
$^3F_2$	14 900	0.21	0.75
$^3H_6$	15 700	0.21	0.035
$^3H_5$	17 700	0.03	—
$^3H_4$	19 700	0.65	0.177
$^1D_2 \rightarrow {}^3F_4, {}^3F_3$	9450	0.27	0.87
$^3H_6$	11 300	0.3	0.034
$^3H_5$	14 050	0.08	0.003
$^3H_4$	16 200	0.35	0.093

4. Conclusions

The optical properties of Pr^{3+} in the $LiTaO_3$ crystal differ from those in $LiNbO_3$ in that the room-temperature visible luminescence originates in both the $^3P_0$ and $^1D_2$ levels whereas the $^3P_0$ luminescence is completely quenched in $LiNbO_3$. The absorption spectrum of $LiTaO_3 : Pr^{3+}$ depends strongly on the polarization of the light incident upon the sample. It can be concluded from the absorption spectra and from results of the group theory assignment that the Pr^{3+} ions enter different sites not of pure C_3 symmetry. Occurrence of the intense luminescence from the $^3P_0$ level to the ground state as well as to higher-lying multiplets makes the $LiTaO_3 : Pr^{3+}$ crystal a promising candidate for a four-level laser material in the visible range.

Acknowledgment

This work was supported by grant No 8T11B06209 of the Polish Committee of Scientific Research (KBN)

References

[1] Miller R C and Nordland W A 1970 *Phys. Rev.* B **2** 4896
[2] Tangonan G L, Barnoski M K, Lotspeich J F and Lee A 1977 *Appl. Phys. Lett* **30** 238
[3] Agostinelli J A and Braunstein G 1993 *Appl. Phys. Lett.* **63** 123
[4] Gitmans F, Sitar Z and Gunter P 1995 *Vacuum* **46** 939
[5] Xie H and Raj R 1993 *Appl. Phys. Lett.* **63** 3146
[6] Amiel O, Cazean P and Salmon R 1995 *J. Mater. Sci.* **30** 3674

[7] Terabe K, Iyi N, Uematsu H and Sakaguchi I 1994 *Proc. 9th IEEE Int. Symp. on Application of Ferroelectrics (New York, 1994)* p 439
[8] Askin A, Boyd G D, Dziedzic J M, Smith R G, Ballman A, Levinstein J and Nassau K 1966 *Appl. Phys. Lett.* **9** 72
[9] Mizuuchi K and Yamamoto K 1995 *Appl. Phys. Lett* **66** 2943
[10] Fan T Y, Cordova-Plaza A, Digonnet M J F, Byer R L and Shaw M J 1986 *J. Opt. Soc. Am.* B **3** 140
[11] Gill D M, Judy A, McCaughan L and Wright J C 1992 *Appl. Phys. Lett.* **60** 1067
[12] Dominiak-Dzik G, Gołąb S, Pracka I and Ryba-Romanowski W 1994 *Appl. Phys.* A **58** 551
[13] Munoz Santiuste J E, Macalik B and Garcia-Sole J 1993 *Phys. Rev.* B **47** 88
[14] Lorenzo A, Bausa L E and Garcia-Sole J 1995 *Phys. Rev.* B **51** 16 643
[15] Lorenzo A, Jaffrezic H, Roux B, Boulon G, Bausa L E and Garcia Sole J 1995 *Phys. Rev.* B **52** 6278
[16] Thiemann O, Donnerberg H, Wohlecke M and Schirmer O F 1994 *Phys. Rev.* B **49** 5845
[17] Garcia-Sole J, Lou L, Monteil A, Boulon G, Lecocq S, Vergara I, Camarillo E and Cochet-Muchy D 1993 *Eur. J. Solid State Inorg. Chem.* **30** 1049
[18] Abedin K S, Sato M, Ito H, Maeda T, Shimamura K and Fukuda T 1995 *J. Appl. Phys.* **78** 691
[19] Wu X, Zhong M S, Chen X, Meng X and Feng D 1994 *Appl. Phys. Lett.* **65** 1088
[20] Nikl M, Morlotti R, Margo C and Bracco R 1996 *J. Appl. Phys.* **79** 2853
[21] Inbar I and Cohen R E 1996 *Phys. Rev.* B **53** 1193
[22] Iyi N, Kitamura K, Izumi F, Yamamoto J K, Hayashi T, Asano H and Kimura S 1992 *J. Solid State Chem.* **101** 340
[23] Gog Th, Griebenov M and Materlik G 1993 *Phys. Lett.* **181A** 417
[24] Kaplyanskii A A 1964 *Opt. Spectrosc.* **16** 329
[25] Penna A F, Chaves A S, Andrade P R and Porto S P S 1976 *Phys. Rev.* B **13** 4907
[26] Sidorov N V, Melnik N N, Palatnikov M N and Serebryakov Yu A 1995 *Fiz. Tverd. Tela* **37** 3477 (in Russian)
[27] Palatnikov M N, Sandler V A, Serebryakov Yu A, Sidorov N V and Kalinnikov V T 1996 *Ferroelectrics* **175** 183
[28] Babadjanian W G, Gorgescu C, Yonescu K, Kostanian R B, Lupei V, Sanamian T W and Nicogosyan W R 1990 *Izv. Akad. Nauk Arm. Fiz.* **25** 356
[29] Judd B R 1962 *Phys. Rev.* **127** 750
[30] Ofelt G S 1962 *J. Chem. Phys.* **37** 511
[31] Kornienko A A, Kaminskii A A and Dunina E B 1990 *Phys. Status Solidi* b **157** 267
[32] Goldner P and Auzel F 1996 *J. Appl. Phys.* **79** 7972
[33] Henderson B and Imbusch G F 1989 *Optical Spectroscopy of Inorganic Solids* (Oxford: Clarendon)
[34] Malinowski M, Wolski R and Woliński W 1986 *J. Lumin.* **35** 1
[35] McCumber D E 1964 *Phys. Rev.* **136** A954